

6-13-2017

Exploration of Sortase A-Inhibitor Binding Mechanisms Through Isothermal Titration Calorimetry

Eddy Liu

Santa Clara University, eyliu@scu.edu

Follow this and additional works at: http://scholarcommons.scu.edu/bioe_mstr



Part of the [Biomedical Engineering and Bioengineering Commons](#)

Recommended Citation

Liu, Eddy, "Exploration of Sortase A-Inhibitor Binding Mechanisms Through Isothermal Titration Calorimetry" (2017).

Bioengineering Master's Theses. 2.

http://scholarcommons.scu.edu/bioe_mstr/2

This Thesis is brought to you for free and open access by the Engineering Master's Theses at Scholar Commons. It has been accepted for inclusion in Bioengineering Master's Theses by an authorized administrator of Scholar Commons. For more information, please contact rsccroggin@scu.edu.

SANTA CLARA UNIVERSITY

Department of Bioengineering

I HEREBY RECOMMEND THAT THE THESIS PREPARED
UNDER MY SUPERVISION BY

Eddy Liu

ENTITLED

**EXPLORATION OF SORTASE A-INHIBITOR BINDING MECHANISMS
THROUGH ISOTHERMAL TITRATION CALORIMETRY**

BE ACCEPTED IN PARTIAL FULFILLMENT OF THE REQUIREMENTS
FOR THE DEGREE OF

**MASTER OF SCIENCE
IN
BIOENGINEERING**

Zhiwen Zhang

06-13-2017

Thesis Advisor

Date

Yulpp Yee

6/13/17

Department Chair

Date

**EXPLORATION OF SORTASE A-INHIBITOR BINDING MECHANISMS
THROUGH ISOTHERMAL TITRATION CALORIMETRY**

By Eddy Liu

Master's Thesis

Submitted to
the Department of Bioengineering
of
SANTA CLARA UNIVERSITY

in Partial Fulfillment of the Requirements
for the degree of
Master's of Science in Bioengineering

Santa Clara, California

Spring 2017

Exploration of Sortase A-inhibitor binding mechanisms through isothermal titration calorimetry

Eddy Liu

Department of Bioengineering

Santa Clara University

2017

ABSTRACT

The enzyme Sortase A plays a critical role in the virulence of gram-positive bacteria, facilitating their ability to attach to and infect host tissues. Because of its accessible location on the surface of bacteria and in light of the emergence of antibiotic-resistant bacterial strains, Sortase A has become an important target for novel drugs and their associated research. Here we investigate the thermodynamic characteristics and binding mechanism of Sortase A and inhibitors using isothermal titration calorimetry. The results support a two-step, sequential binding mechanism involving induced fit and conformational change. We recommend that further studies involving other small molecule inhibitors be carried out to evaluate the consistency of the proposed binding mechanisms. Additionally, it may be worthwhile to develop Sortase A inhibitors which mimic peptides given the variable and flexible structure of its active site.

TABLE OF CONTENTS

<u>Section</u>	<u>Page Number</u>
Abstract	i
Table of Contents	ii
List of Figures	iii
List of Tables	iv
Introduction	1-6
Materials and Methods	7-10
<i>Sortase A $\Delta N59$ Expression and Purification</i>	7-8
<i>ITC Experiments</i>	8-10
Results	11-18
Discussion	19-24
Conclusion	25
References	26-27
Supplementary Data	28-32

LIST OF FIGURES

<u>Figure</u>	<u>Page Number</u>
Figure 1 – Sortase A, schematic diagram	2
Figure 2 – Actarit, chemical structure	3
Figure 3 – Isothermal titration calorimeter, schematic diagram	4
Figure 4 – Sample ITC binding isotherm, 0.4 mM EDTA, 5 mM CaCl ₂	5
Figure 5 - ITC binding isotherm (1 of 3), 19 μM Sortase A ΔN59, 380 μM Actarit	12
Figure 6 - ITC binding isotherm (2 of 3), 19 μM Sortase A ΔN59, 380 μM Actarit	13
Figure 7 - ITC binding isotherm (3 of 3), 19 μM Sortase A ΔN59, 380 μM Actarit	14
Figure 8 - ITC binding isotherm, 1 μM Sortase A ΔN59, 1 mM Actarit	16
Figure 9 - ITC binding isotherm, 1 μM Sortase A ΔN59, 5 μM Actarit	17
Figure 10 – Two-site sequential binding model, Sortase A monomer and Actarit	20
Figure 11 – Two-site sequential binding model, Sortase A homodimer and Actarit	20
Figure 12 – ITC binding isotherm, model fit by hand	22
Figure S1 – Raw ITC binding isotherm (1 of 3), 19 μM Sortase A ΔN59, 380 μM Actarit	28
Figure S2 – Raw ITC binding isotherm (2 of 3), 19 μM Sortase A ΔN59, 380 μM Actarit	29
Figure S3 – Raw ITC binding isotherm (3 of 3), 19 μM Sortase A ΔN59, 380 μM Actarit	30
Figure S4 – Representative raw experimental ITC data, 19 μM Sortase A ΔN59, 380 μM Actarit	31
Figure S5 – Raw experimental ITC data, 1 μM Sortase A ΔN59, 5 μM Actarit	32

LIST OF TABLES

<u>Table</u>	<u>Page Number</u>
--------------	--------------------

Table 1 – Summary of calculated values from three repeated ITC experiments, 19 μ M Sortase A Δ N59, 380 μ M Actarit	15
---	----

INTRODUCTION

Recently, methicillin-resistant *Staphylococcus aureus* (MRSA) has become a growing health concern due to its role in hospital-related infections¹. This has led to increasing interest in developing new antibiotics which target *S. aureus* and other related gram-positive bacterial pathogens without directly killing or inhibiting their growth. Such an approach would reduce the probability of applying a selective evolutionary pressure that would promote their development of new resistance mechanisms².

The enzyme Sortase A is a membrane-bound cysteine transpeptidase utilized by *S. aureus* and many other gram-positive pathogens to anchor surface proteins to their cell walls³. These exterior surface proteins play critical roles in bacterial adhesion to and invasion of host cells, making them indispensable tools for bacterial virulence. Surface proteins destined for anchoring to the cell wall possess a cell wall sorting signal, consisting of an LPXTG motif at the end of their C-terminal chain. Membrane-bound Sortase A recognizes this peptide motif and cleaves it between the T and G residues, followed by the formation of a thioester acyl-enzyme intermediate and subsequent covalent attachment to a pentaglycine unit of the cell wall molecule lipid-II⁴ (see Figure 1 for schematic representation). Multiple studies have shown that loss or absence of Sortase A function renders *S. aureus* significantly much less capable of infecting host tissues⁵⁻⁷.

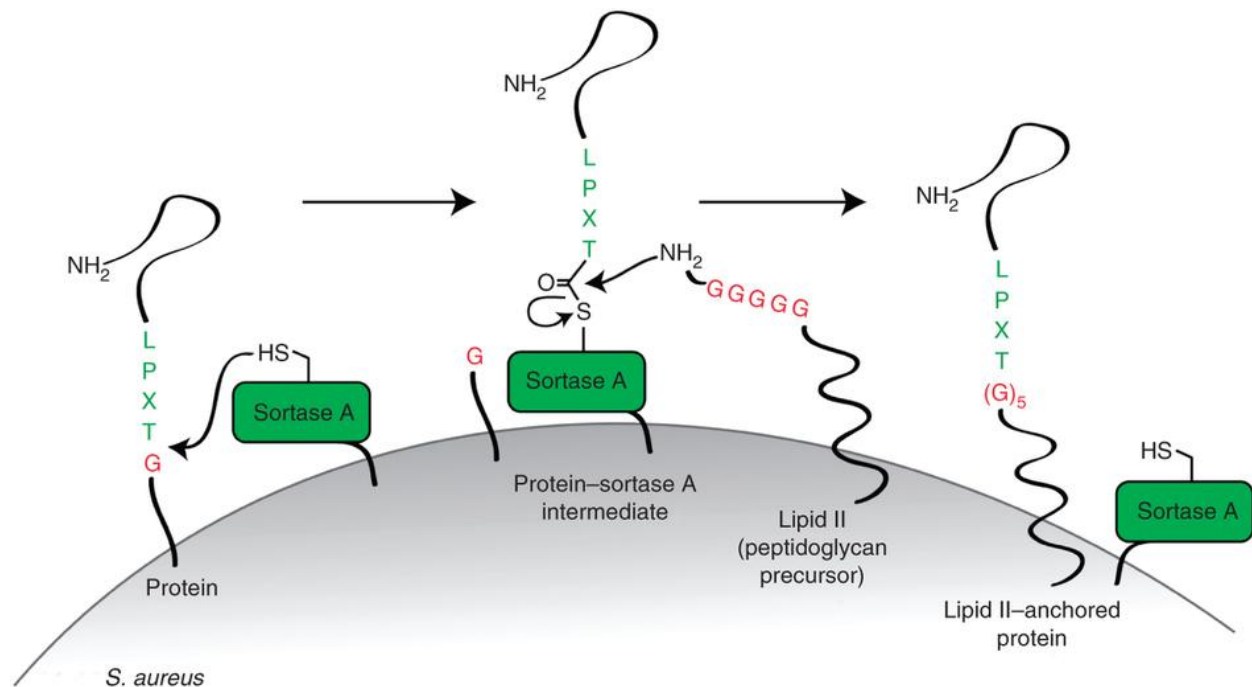


Figure 1.

Schematic diagram of how Sortase A anchors proteins to the cell wall of gram-positive bacteria. Figure from *Site-specific C-terminal and internal loop labeling of proteins using sortase-mediated reactions* by Guimaraes et al.¹⁷

Due to its accessible location on the exterior surface of gram-positive bacteria, Sortase A is a promising drug target for new antibiotics and inhibitor compounds. In addition, selective targeting of bacterial Sortase A is feasible as there are no known eukaryotic i.e. mammalian sortase equivalents⁸. To date, many potential Sortase A inhibitors have been identified and developed using several different techniques, most commonly via high-throughput screening of synthetic or natural compound libraries in addition to virtual screening approaches⁹.

Development of a suitable Sortase A inhibitor has required detailed information regarding the structure and mechanism of function of the enzyme itself. Although much data has been generated in multiple, there remains some uncertainty over the binding mechanism of Sortase A with substrate, especially under *in vivo* conditions. To elucidate some aspects of that binding mechanism, this study utilized isothermal titration calorimetry (ITC) to study the interactions

between Sortase A and Actarit, a chemical compound originally developed for use as rheumatoid arthritis drug¹⁰ (see Figure 2). Actarit had previously been identified via high-throughput screening as a potential Sortase A inhibitor molecule with an IC₅₀ value of 20 μM (data not yet published).

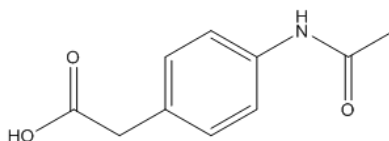


Figure 2.

Chemical structure of Actarit, a disease-modifying anti-rheumatic drug used to slow down the progression of rheumatoid arthritis. Prior *in vivo* studies have demonstrated its potential use as an inhibitor of Sortase A.

Isothermal titration calorimetry (ITC) is a useful quantitative *in vitro* approach to measure the heat generated or absorbed in a titration experiment between a macromolecule and a ligand. ITC experiments are conducted in an isothermal titration calorimeter (also known as an ITC machine), which automatically conducts a titration experiment and measures the heat of reaction upon each injection of ligand into a sample of macromolecule (see Figure 3 for schematic of an ITC machine).

The isothermal titration calorimeter contains two identical cells, one serving as a reference cell, and the other being the sample cell. The reference cell always has constant power (a reference power) being applied to it, maintaining it at constant temperature. Sample containing macromolecule to be studied is injected into the sample cell. During an ITC experiment, ligand is titrated into the sample cell in precise aliquots. Upon molecular interaction of the ligand and macromolecule in solution, heat is either generated or taken up, depending on the nature of the reaction. Sensitive temperature-sensing circuits detect differences in temperature between the reference cell and the sample cell, and will either add or withdraw heat to keep both cells at the same temperature. An exothermic reaction (heat being released) would increase the temperature of the sample cell, and power to the reference cell will be decreased to maintain equal temperature between the two cells. In a similar fashion, an endothermic reaction (heat being

taken up) would decrease the sample cell temperature, and power to the reference cell will be increased to maintain that constant temperature (hence the term ‘isothermal’ in isothermal titration calorimetry).

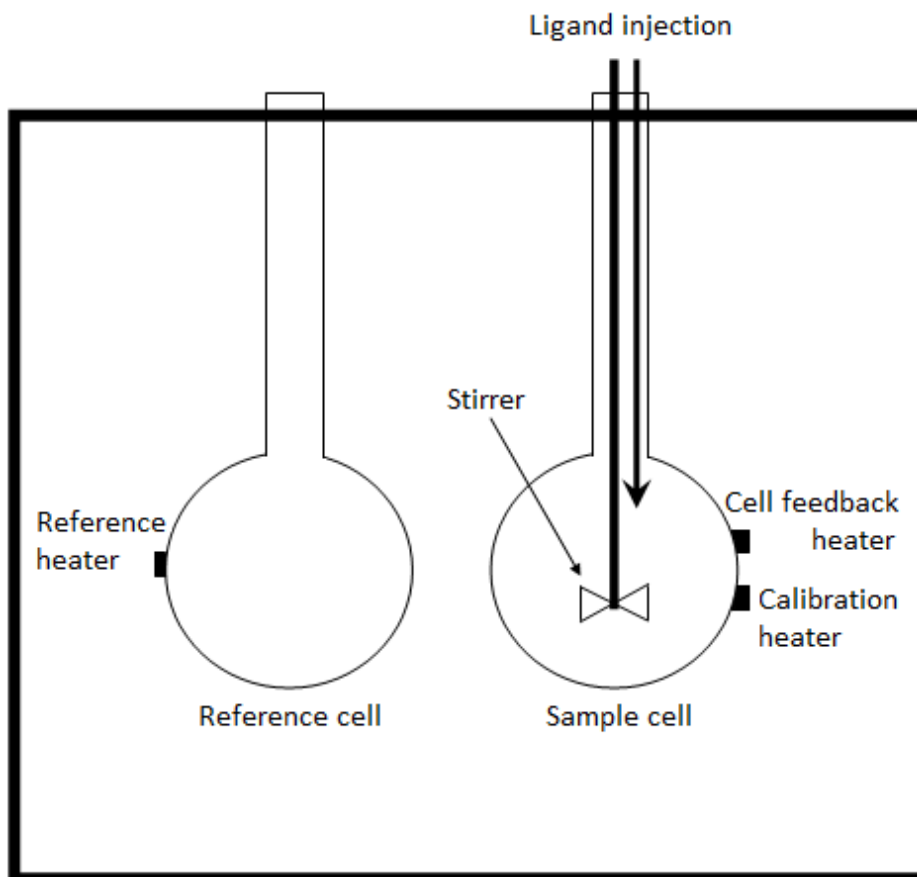


Figure 3.

Schematic diagram of the interior of an isothermal titration calorimeter.

The control software used to operate the ITC machine plots the amount of power needed to maintain the reference and sample cells at constant temperature upon each titration (injection) of ligand against time. This experimental raw data is displayed as a series of spikes, with each spike corresponding to one ligand injection (See Figure S4 in Supplementary Data for a representative plot). The spikes are integrated with respect to time, which gives the total amount of heat (ΔH) produced for each injection. When plotted against the molar ratio of ligand to macromolecule, analysis of patterns in the binding isotherm plot can provide clues as to the nature of binding

interaction between the macromolecule and the ligand (see Figure 4 for sample plot). Each data point corresponds with one injection of ligand into the sample of macromolecule, just as in the experimental raw data.

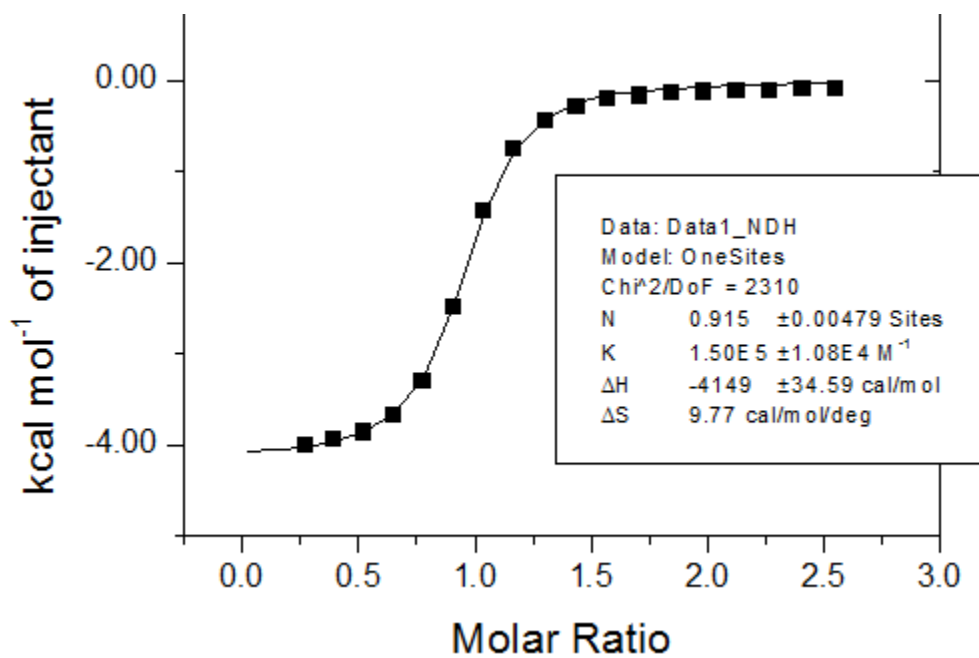


Figure 4.

Sample ITC binding isotherm of EDTA (0.4 mM) and CaCl₂ (5 mM) at 25°C. A total of 19 injections of 2 μl were carried out, with the first data point removed for being an outlier. Solid black line represents a global fit using a one-site binding model. Values for changes in enthalpy (ΔH), entropy (ΔS), and binding constant (K) are shown in the boxed area and were automatically calculated by fitting of the binding model.

ITC binding isotherms of molecular species demonstrating exothermic interactions often produce sigmoid curves, as depicted above. As an example, in Figure 4, the 2nd to 5th data points form a relatively shallow slope (the first data point has been omitted due to being an outlier; it is not shown). This corresponds to a very low concentration of ligand (CaCl₂) interacting exothermically with binding sites on the macromolecule (EDTA). The 6th to 10th data points show much larger amounts of heat being generated, as evidenced by the significantly increased slope of the plot. This reflects that upon each subsequent injection of ligand, the ligand to macromolecule molar ratio is also being raised. It should come as no surprise that increased

availability of ligand in the sample cell correlates with increased generation of heat due to the exothermic nature of the binding interactions between the ligand and macromolecule. Finally, in the remaining 11th to 19th data points, the slope tapers off and plateaus due to the fact that the macromolecules' binding sites have become increasingly saturated with ligand. With increasingly fewer and fewer unoccupied binding sites available for interaction with ligand, the change in enthalpy (heat) decreases, as reflected in the shallower slope. In other words, less molecular interaction between ligand and macromolecule results in smaller changes in enthalpy, all of which is accurately detected by the ITC machine.

As a final note, it should be noted that the molar ratio as displayed on the graph does not directly correspond to actual stoichiometries of the interacting species. Even though it appears in the example graph above (Figure 4) that EDTA is saturated with CaCl₂ when the CaCl₂ to EDTA ratio is roughly 2.0, this does not necessarily mean that EDTA has exactly two binding sites. All the molar ratio can show is that upon completion of the ITC experiment (all injections), the total ligand to macromolecule ratio reached ~2.5 with regards to everything contained in the sample cell. It does not mean that all ligand is now bound to macromolecule.

From a single ITC experiment it is possible to determine changes in enthalpy (ΔH), binding affinity (K_a), and binding stoichiometry (n) of the macromolecule-ligand interaction. From these initial measurements, values for changes in Gibbs free energy (ΔG) and changes in entropy (ΔS) can also be calculated using the following equation:

$$\Delta G = -RT \ln K_a = \Delta H - T\Delta S$$

ITC's ability to characterize the thermodynamics of binding interactions between macromolecules (e.g. proteins) and ligands (e.g. small molecules or peptides) allows for the development and optimization of compounds in drug discovery.

MATERIALS AND METHODS

Sortase A $\Delta N59$ Expression and Purification

A subculture of Sortase A $\Delta N59$ (with C-terminal 6xHis tag) was made by picking some cells from a previously made glycerol stock (kept at -80°C) and inoculating them in 10 ml of LB containing 50 $\mu\text{g/ml}$ kanamycin. This starter culture was allowed to grow overnight at 37°C in a shaking incubator set at 225 rpm.

The next day the starter culture was added to 990 ml of pre-autoclaved LB in a 1 liter Erlenmeyer flask (also pre-autoclaved). Kanamycin was added to a final concentration of 50 $\mu\text{g/ml}$. This was allowed to incubate at 37°C in a shaking incubator set at 225 rpm. OD_{600} readings were periodically taken by pulling a small sample from the culture and checking it using a photo spectrometer. When OD_{600} reached approximately 0.6, the cells were induced with IPTG (final concentration 10 μM). At this point, the incubator temperature was lowered to 23°C and the culture was allowed to grow overnight.

The culture was aliquoted into 50 ml centrifuge tubes, and centrifuged at 5,000 rpm for 10 minutes at 4°C to pellet the cells. The supernatant was discarded. The tubes were massed to obtain a rough estimate of the amount of bacteria produced (wet weight). The cell pellets were re-suspended in lysis buffer (PBS, pH 7.4 + 15 mM imidazole) at roughly 4 ml lysis buffer per gram of cell. All the re-suspended cells were consolidated into a single 50 ml centrifuge tube. Lysozyme was added to a final concentration of 1 mg/ml and the solution was thoroughly mixed by pipette. It was allowed to incubate on ice for 30 minutes. Afterwards the solution was sonicated to ensure complete cell lysis (20 cycles of 10 seconds 'on' followed by 15 seconds 'off'). The sonicated solution was then transferred to thick-walled centrifuge tubes and centrifuged at 16,000 rpm for 40 minutes at 4°C in a floor centrifuge.

500 μl of HisPur Ni-NTA Resin (Thermo Scientific) was placed in a 15 ml centrifuge tube. It was re-suspended in 5 ml of wash buffer (PBS, pH 7.4 + 25 mM imidazole) and centrifuged at 2,000 rpm for 5 minutes. The supernatant was discarded. This washing step was repeated two

additional times. The centrifuged solution from above was then added to the Ni-NTA slurry and allowed to incubate overnight at 4°C.

The following day the mixture was centrifuged at 2,000 rpm for 20 minutes at 4°C to sediment the Ni-NTA resin. The supernatant was discarded. The resin beads were re-suspended in 5 ml of wash buffer and centrifuged at 2,000 rpm for 10 minutes at 4°C. The supernatant was discarded. This washing process was repeated an additional 5 times.

The protein was eluted from the Ni-NTA resin beads by re-suspending the beads in 1 ml of elution buffer (PBS, pH 7.4 + 250 mM) and centrifuging at 2,000 rpm for 10 minutes at 4°C. To evaluate the purity of the protein sample, a small sample was run on a 12% SDS-PAGE gel under denaturing conditions and visualized using LabSafe GEL Blue™ (G-Biosciences).

Dialysis was performed to remove the imidazole and concentrate the purified protein in PBS. Dialysis tubing was pre-soaked in deionized water for 15 minutes. The inside of the tubing was washed with DI water. After clamping one end of the tubing, the protein sample was added, and the other end was clamped while allowing for the presence of a small pocket of air inside for buoyancy. This was submerged in 500 ml of PBS (pH 7.4) in a 1 liter beaker overnight with moderate stirring by magnetic stir bar. Afterwards the protein sample was retrieved and transferred to 1.5 ml micro centrifuge tubes. Protein concentration was determined via Nanodrop. Protein samples were stored at -20°C when not in use.

ITC Experiments

All ITC experiments were performed in a MicroCal™ iTC₂₀₀ system (Malvern). The buffer bottle was simply filled with DI water, as was the bottle intended to hold distilled water. The methanol bottle was filled with methanol. When not normally in use, both the sample and reference cells of the ITC system were filled with approximately 300 µl of DI water. All manual loading and emptying steps were performed with a 3 inch Hamilton syringe.

Before each ITC experiment, the sample cell was emptied via syringe and the cell cleaning device was inserted. On the 'Instrument Controls' tab of the ITC200 control software, the jacket temperature was set to 25°C (under 'Thermostat Control'). Using the 'Accessory Station', a 'Cell and Syringe Wash' was performed, followed by a 'Cell Water Rinse (Long)'. Residual liquid from the cell cleaning process was manually removed by syringe. DI water was used to clean the syringe before and/or following each step requiring manual syringe use.

Afterwards, the sample cell was filled with 300 µl of protein sample (e.g. Sortase A ΔN59 in PBS, pH 7.4). Following recommended guidelines outlined in the system operating instructions, introduction of air bubbles into the sample cell was avoided to the best extent possible, and any excess sample was removed from the top of the cell. Meanwhile, 100 µl of ligand sample (e.g. Actarit in PBS, pH 7.4) was added to a clean PCR tube and this tube was placed in the sample holder. The auto-pipette was filled with this ligand sample following the walkthrough initiated upon selecting the 'Syringe Fill' button under the 'Accessory Station'. Once the ITC system had settled at 25°C, the auto-pipette was carefully lowered in to the sample cell.

On the 'Advanced Experimental Design' tab, parameters of the ITC program were adjusted to those required by the experiment. Parameters used for all ITC experiments are listed below.

Experimental Parameters

Total number of injections: 19

Cell temperature (°C): 25

Reference power: 0

Initial delay (sec): 60

Syringe concentration: Varies (Actarit)

Cell concentration: Varies (Sortase A ΔN59)

Stirring speed (rpm): 750 (the maximum allowed for a twisted paddle, used in these experiments)

Feedback mode/gain: High

Injection Parameters

Volume (μl): 2

Duration (sec): 4

Spacing (sec): 180

Filter period (sec): 5

A unique file name was given to each ITC experiment. To begin the ITC experiment, 'Start' was selected on the control panel and the experiment was allowed to progress automatically.

Following the conclusion of each experiment, the sample cell was manually emptied, the cell cleaning device inserted, and a 'Cell and Syringe Wash' was performed, followed by a 'Cell Water Rinse (Long)'. As usual, residual liquid from the cell cleaning process was manually removed by syringe.

ITC data gathered from each individual 'run' was analyzed using included Origin® data scientific plotting software. After starting the program, 'Read Data' was selected underneath 'ITC Main Control' and the appropriate ITC raw data file opened. By default the 'DeltaH' window is shown, which plots kcal per mole of injectant versus the molar ratio of ligand to macromolecule. Any data points suspected of being clear outliers was removed using the 'Remove Bad Data' button under 'Data Control'.

Afterwards, a 2-site, sequential binding sites model was fitted by clicking on 'Sequential Binding Sites' under 'Model Fitting'. ('2' was entered upon being prompted for number of sites). In the 'Fitting Function Parameters' dialog box, '100 Iter.' was clicked to perform up to 100 Levenberg-Marquardt iterations to achieve optimal curve fit (until the Chi^2 value no longer decreases). After clicking 'Done', a small text box containing the fitting parameters appears and its contents noted down.

To create figures for visual analysis, 'Final Figure' was selected from the 'ITC' menu. The box containing fitting parameters was copied over from the previous step to be alongside the graphs.

RESULTS

ITC experiments involving the titration of 380 μM Actarit into 19 μM Sortase A ΔN59 were carried out for a total of three times, in addition to other molar ratio combinations of Actarit and Sortase A ΔN59 . This molar proportion of Sortase A and Actarit was chosen after multiple ITC experiments with various molar ratios were done to optimize generation of a full binding curve over 19 injections as well as ensuring that all potential binding sites on Sortase A were saturated with Actarit. All of the following results were derived from ITC experiments performed on a MicroCal™ iTC200 system (by Malvern) with identical experimental parameters as follows (except for absolute concentrations of Actarit and Sortase A ΔN59 , which vary with each experiment):

- A total of 19 injections of 2 μl volume each, with 4 second duration, 180 second spacing, and a 5 second filter period
- Cell temperature set at constant 25°C
- Reference power set at 0
- Initial delay of 60 seconds
- Stirring speed set at 750 rpm, the maximum allowable for a twisted paddle, used in these experiments
- Feedback mode/gain set to 'High'

All experimental results were analyzed using the included Origin® data analysis software. Various binding models were fitted onto the generated ITC binding isotherm plots, which graph kcal/mol of ligand (Actarit) over the molar ratio of ligand to macromolecule (Actarit to Sortase A ΔN59). One-site, two-site, and three different sequential binding site models (one to three sites) were fitted to the data. Of these attempted binding models, it was found that the two-site, sequential binding model provided the best fit for all data sets, as determined by the minimal calculated $\chi^2/\text{degrees of freedom}$ values. The binding isotherms from these experiments along with their fitted binding models are depicted in Figures 5-7.

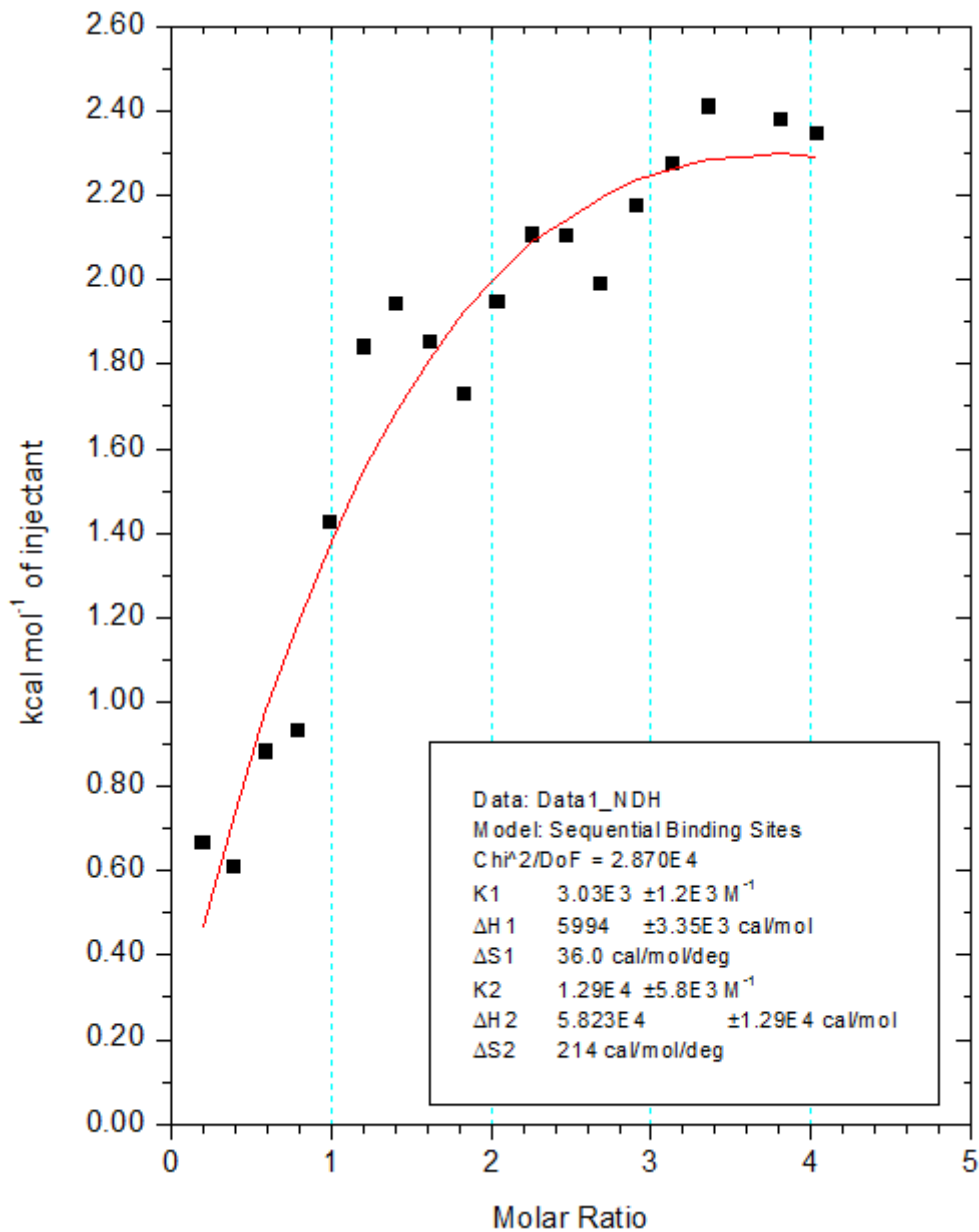


Figure 5.

ITC binding isotherm of Sortase A ΔN59 (19 μM) and Actarit (380 μM) at 25°C (first of three experimental repetitions). Data point corresponding to the 17th of 19 total injections has been removed (See Supplementary Data Figure S1 for full data set). Solid red line corresponds to global fit using two-site sequential binding model. Values for changes in enthalpy (ΔH1, ΔH2), entropy (ΔS1, ΔS2), and binding constants (K1, K2) are shown in the boxed area and were automatically calculated by fitting of the binding model.

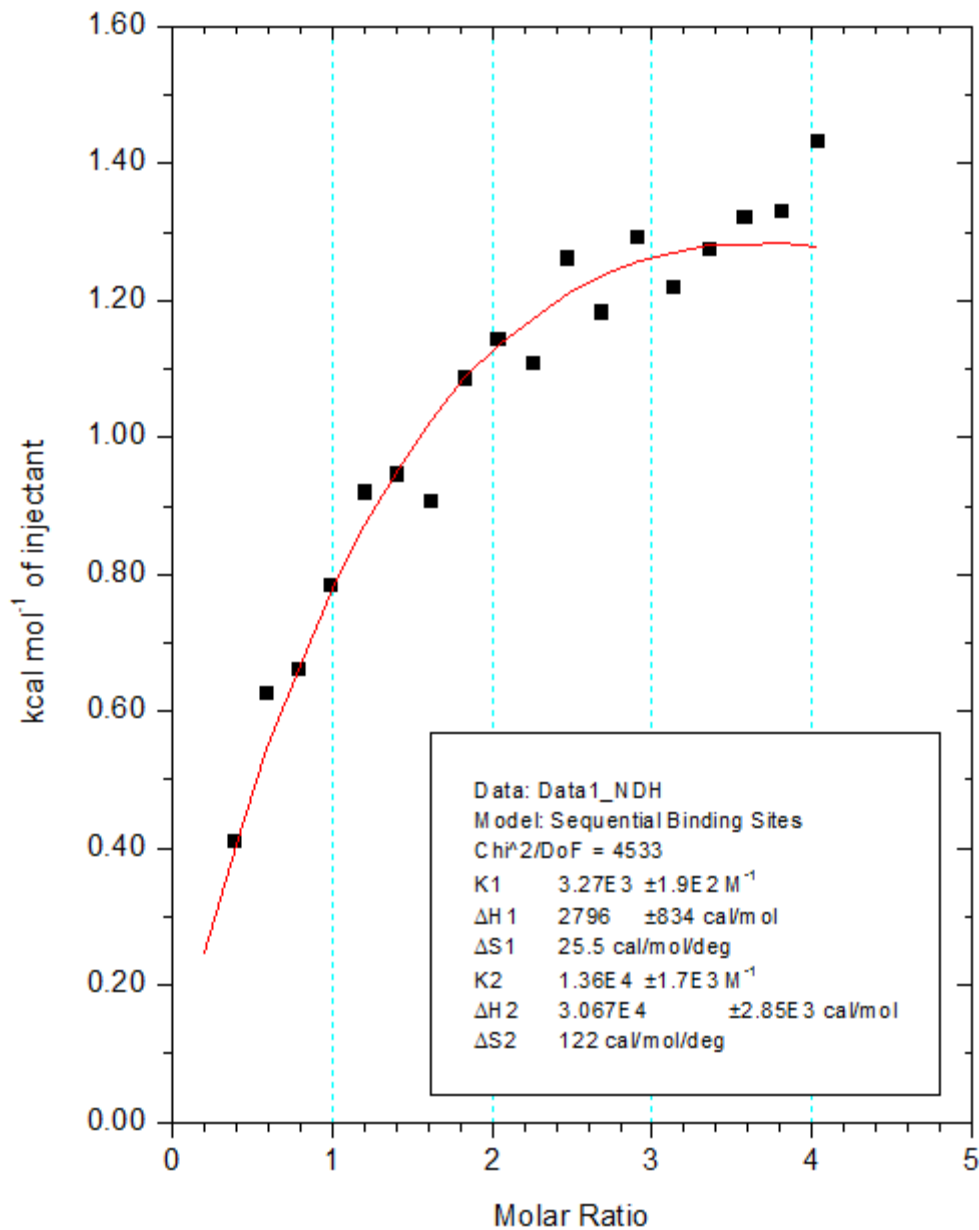


Figure 6.

ITC binding isotherm of Sortase A ΔN59 (19 μM) and Actarit (380 μM) at 25°C (second of three experimental repetitions). Data point corresponding to the 1st of 19 total injections has been removed (See Supplementary Data Figure S2 for full data set). Solid red line corresponds to global fit using two-site sequential binding model. Values for changes in enthalpy (ΔH1, ΔH2), entropy (ΔS1, ΔS2), and binding constants (K1, K2) are shown in the boxed area and were automatically calculated by fitting of the binding model.

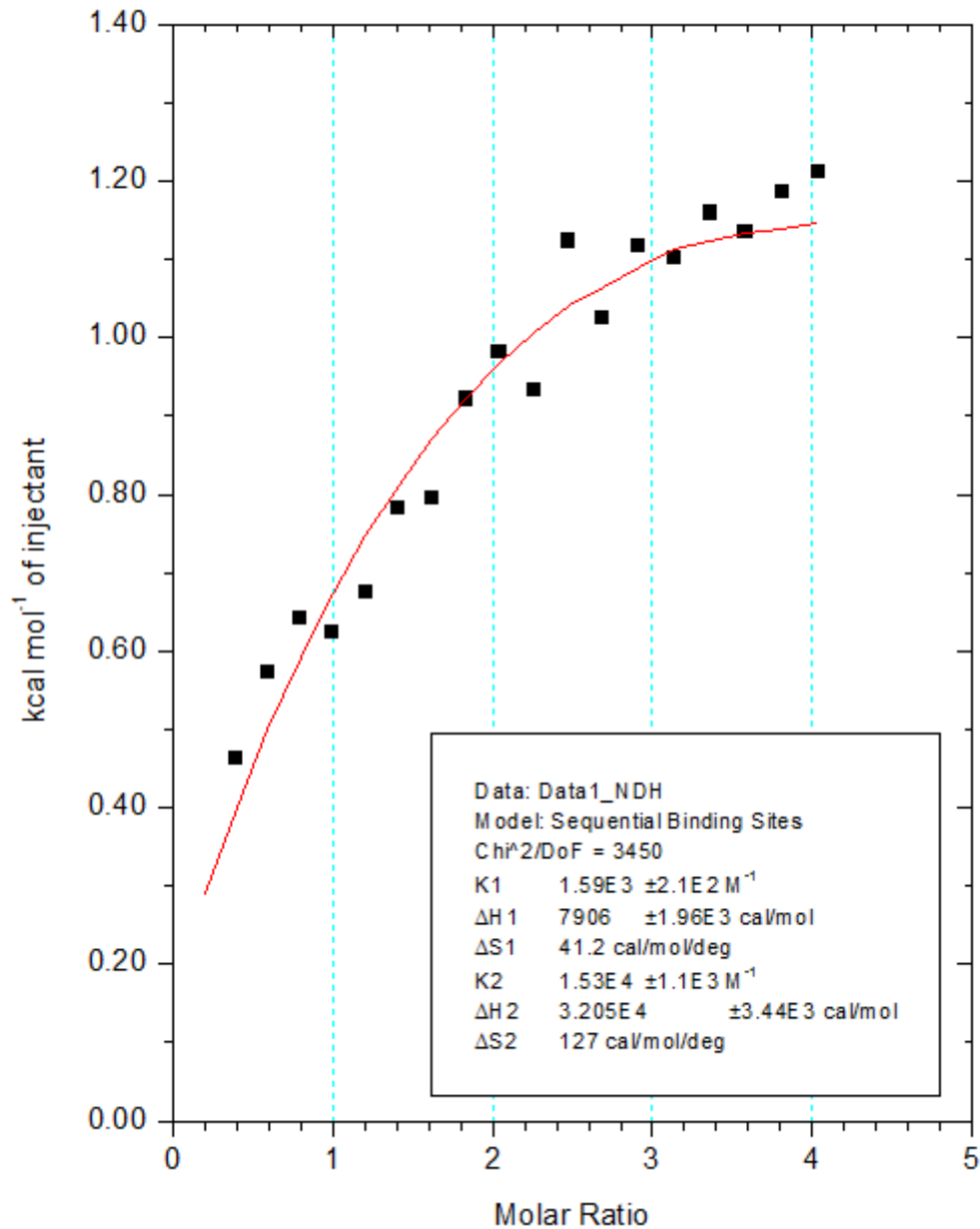


Figure 7.

ITC binding isotherm of Sortase A ΔN59 (19 μM) and Actarit (380 μM) at 25°C (third of three experimental repetitions). Data point corresponding to the 1st of 19 total injections has been removed (See Supplementary Data Figure S3 for full data set). Solid red line corresponds to global fit using two-site sequential binding model. Values for changes in enthalpy (ΔH1, ΔH2), entropy (ΔS1, ΔS2), and binding constants (K1, K2) are shown in the boxed area and were automatically calculated by fitting of the binding model.

Figures 5 through 7 above show the resultant binding isotherms of three repeated ITC experiments involving the titration of 380 μM Actarit into 19 μM Sortase A ΔN59 . This molar ratio combination results in final ligand to macromolecule ratios of approximately four. Each data point (save for those not shown due to being omitted as outliers) corresponds to one injection of Actarit into the sample cell containing Sortase A ΔN59 . The red lines depict two-site sequential binding models as fitted by the Origin® analysis software. Values listed in the boxed areas report calculated changes in enthalpy (ΔH1 , ΔH2), entropy (ΔS1 , ΔS2), and binding constants (K1 , K2). These are automatically generated by the analysis software after selection of the desired binding model, and are summarized below in Table 1:

Repetition Num.	1	2	3	Average
$\text{K1 (M}^{-1}\text{)}$	$3.03 * 10^3$	$3.27 * 10^3$	$1.59 * 10^3$	$2.63 * 10^3$
$\Delta\text{H1 (cal/mol)}$	$5.99 * 10^3$	$2.80 * 10^3$	$7.91 * 10^3$	$5.57 * 10^3$
$\Delta\text{S1 (cal/mol/deg)}$	36.0	25.5	41.2	34.2
$\text{K2 (M}^{-1}\text{)}$	$1.29 * 10^4$	$1.36 * 10^4$	$1.53 * 10^4$	$1.39 * 10^4$
$\Delta\text{H2 (cal/mol)}$	$5.82 * 10^4$	$3.07 * 10^4$	$3.21 * 10^4$	$4.03 * 10^4$
$\Delta\text{S2 (cal/mol/deg)}$	$2.14 * 10^2$	$1.22 * 10^2$	$1.27 * 10^2$	$1.54 * 10^2$
$\text{K1}_d (\mu\text{M)}$	330	306	629	422
$\text{K2}_d (\mu\text{M)}$	77.5	73.5	65.3	72.1

Table 1.

Calculated values for changes in enthalpy (ΔH1 , ΔH2), entropy (ΔS1 , ΔS2), and binding constants (K1 , K2) resulting from the fitting of a two-site, sequential binding model to data sets generated from ITC experiments involving the titration of 380 μM Actarit into 19 μM Sortase A ΔN59 at 25°C. Dissociation constants (K1_d and K2_d) were calculated by taking the inverse of their respective binding constants (K1 and K2).

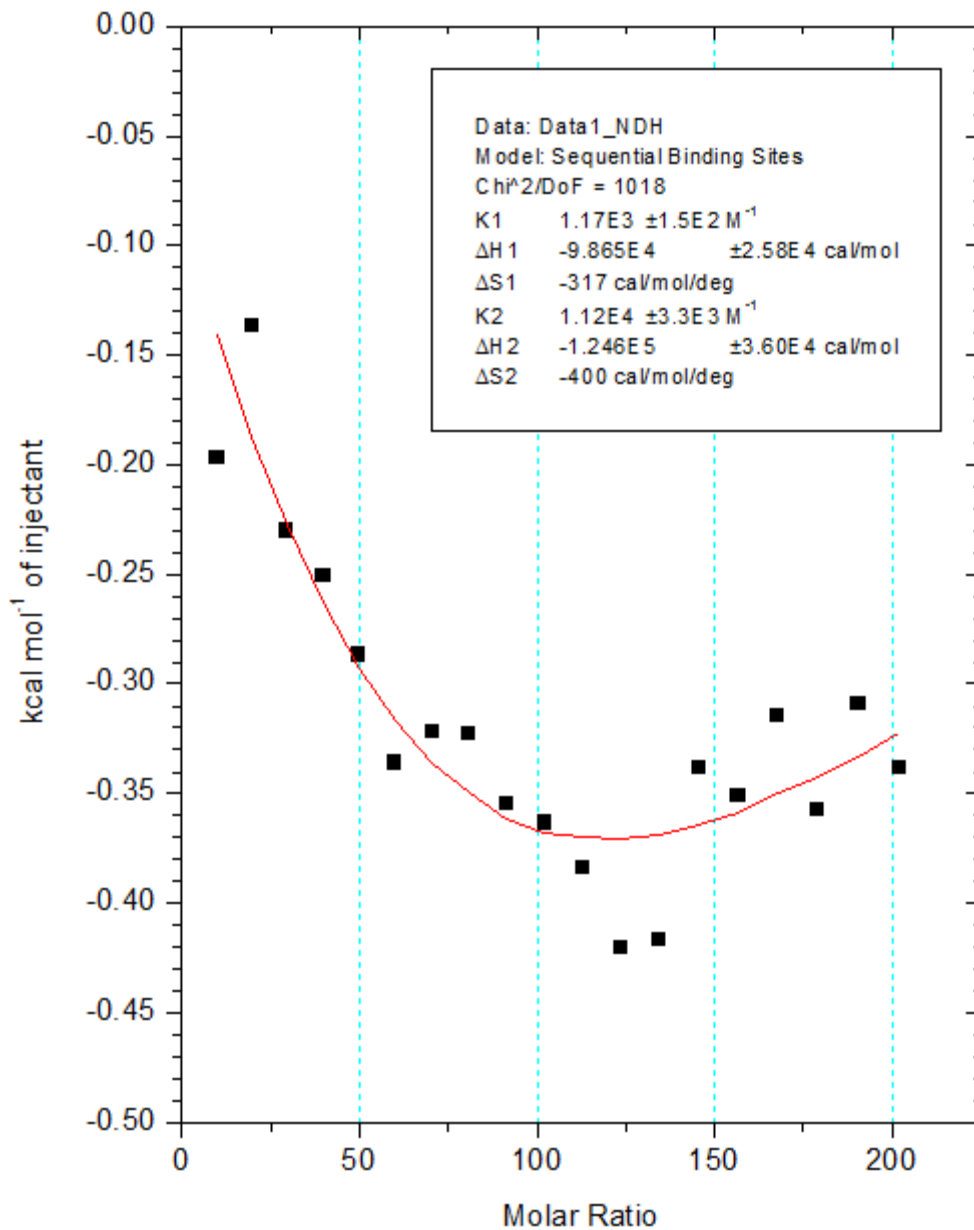


Figure 8.

ITC binding isotherm of Sortase A ΔN59 (1 μM) and Actarit (1 mM) at 25°C. Solid red line corresponds to global fit using two-site sequential binding model. Values for changes in enthalpy (ΔH1, ΔH2), entropy (ΔS1, ΔS2), and binding constants (K1, K2) are shown in the boxed area and were automatically calculated by fitting of the binding model.

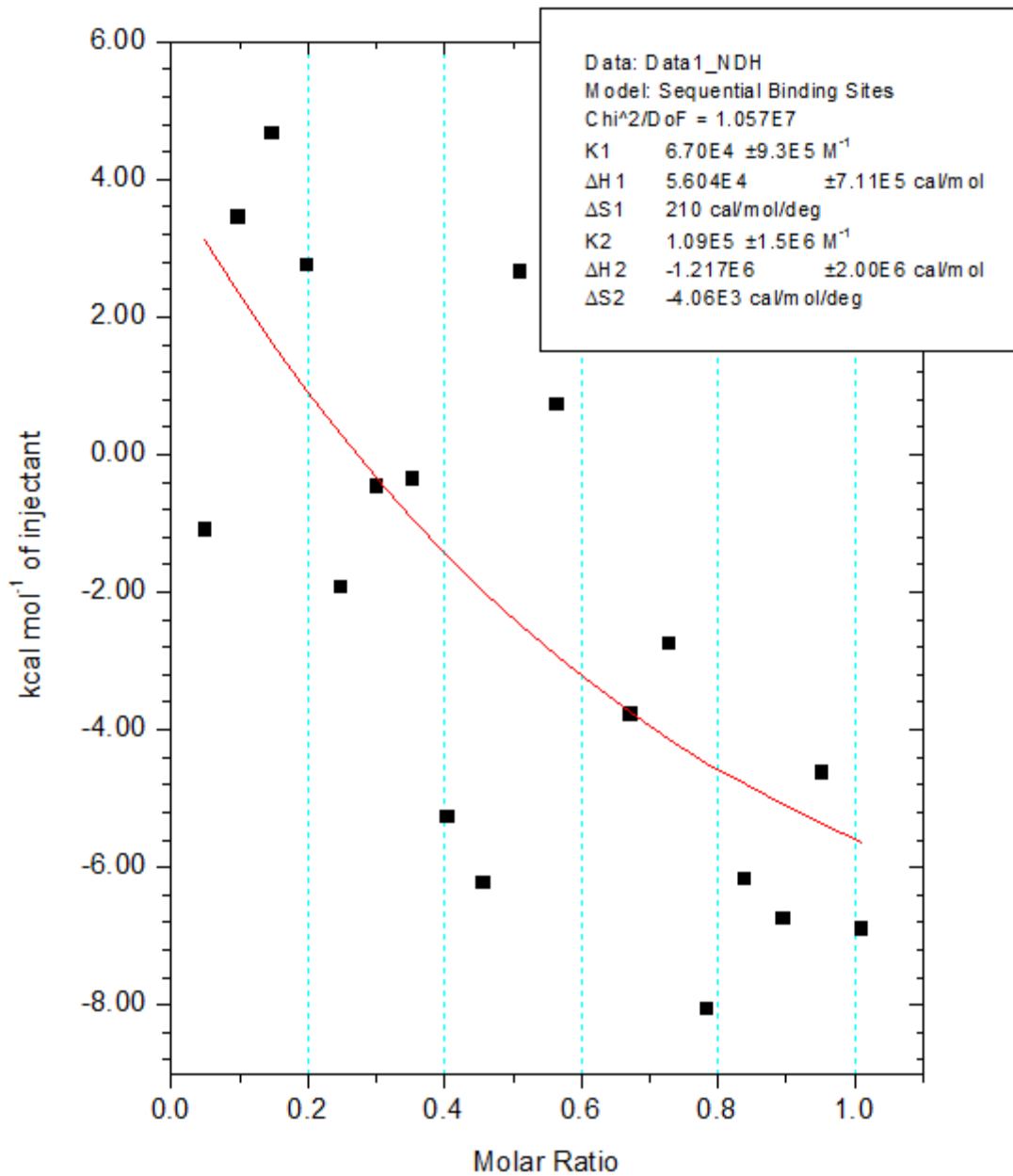


Figure 9.

ITC binding isotherm of Sortase A ΔN59 (1 μM) and Actarit (5 μM) at 25°C. Data point corresponding to the 1st of 19 total injections has been removed. Solid red line corresponds to global fit using two-site sequential binding model. Values for changes in enthalpy (ΔH1, ΔH2), entropy (ΔS1, ΔS2), and binding constants (K1, K2) are shown in the boxed area and were automatically calculated by fitting of the binding model.

Figures 8 and 9 above show two different binding isotherms representative of ITC binding isotherms with different molar concentrations of Actarit and Sortase A Δ N59. Both of these ITC experiments were conducted using the same exact experimental parameters as those previously described, except for the varied sample concentrations of ligand and macromolecule. Figure 8 plots the experimental results of the titration of 1 mM Actarit into 1 μ M Sortase A Δ N59, giving a final ligand to macromolecule ratio of approximately 200. Figure 9 plots the experimental results of the titration of 5 μ M Actarit into 1 μ M Sortase A Δ N59, giving a final ligand to macromolecule ratio of approximately 1.0. Each data point (save for those not shown due to being omitted as outliers) corresponds to one injection of Actarit into the sample cell containing Sortase A Δ N59. The red lines depict two-site sequential binding models as fitted by the Origin® analysis software. Values listed in the boxed areas report calculated changes in enthalpy (Δ H1, Δ H2), entropy (Δ S1, Δ S2), and binding constants (K1, K2).

DISCUSSION

As displayed in Figures 5 through 7 above, the binding isotherms for the three repeated experiments of 380 μM Actarit and 19 μM Sortase A ΔN59 generally show upward trends and positive slopes. These indicate that overall, the interaction between Actarit and Sortase A ΔN59 is exothermic in nature and therefore thermodynamically favorable. Software analysis of data from multiple ITC experiments has demonstrated that fitting of a two-site sequential binding model results in the lowest $\chi^2/\text{degrees of freedom}$ values when compared to other alternative binding models. Interestingly, this was found to hold true regardless of what combinations of Actarit and Sortase A ΔN59 concentrations were used in experimental setups.

A two-site sequential binding model implies that binding interactions between ligand and macromolecule involve two separate binding steps, the second of which cannot occur until the first one has happened first. This binding model differs from a two-site binding model in that the two binding sites are not independent i.e. there exists some synergistic effects between the two. It may also imply that the occurrence of molecular binding at the first site changes the physical properties of the macromolecule in such a way that the second binding site now exhibits different properties than had the first binding event not occurred. This is why calculated values for changes in enthalpy (ΔH), entropy (ΔS), and binding constants (K) come in pairs in the case of two-site binding models. It is also the reason why the same parameters for the two binding events are not equivalent when dealing with non-independent or sequential binding models.

Previous work has shown that Sortase A *in vitro* exists in an equilibrium state between monomer and homodimer with a dissociation constant K_d of 55 μM^{11} . Given that the concentration of Sortase A in the ITC experiments is only 19 μM , we can assume that the majority of Sortase A exists in monomer form, with only a small fraction forming homodimers. Additionally, the relationship of the calculated binding constants as listed in Table 1 above ($\text{K}_2 > \text{K}_1$) suggests a positively cooperative binding model, i.e. the second binding event is stronger than the first one and therefore more favorable. Taking a two-site sequential binding model into consideration, one possible binding mechanism is as follows (Figure 10):

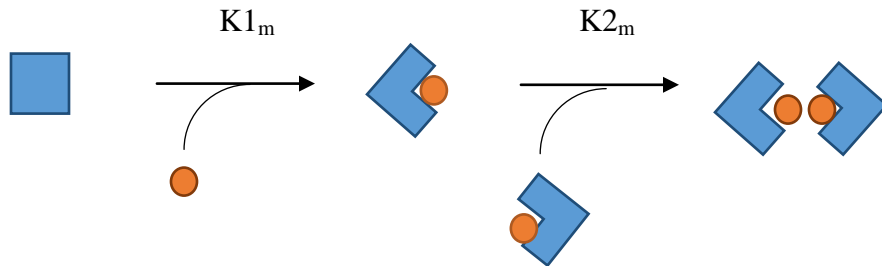


Figure 10.

Two-site sequential binding model for the binding of Actarit (oval) to monomeric Sortase A (square ‘unbound’ and notched square ‘bound’). Binding constants for the first and second binding events are $K1_m$ and $K2_m$ respectively.

In the first binding step, a molecule of Actarit binds to the active site of a monomeric Sortase A. This first binding event may induce a conformational change in the structure of Sortase A monomer which makes it more conducive to forming a dimer with another similarly bound monomer, forming a homodimer. This would be interpreted as the second binding event. The experimental data (see Table 1 for summary of values) strongly suggests that within the two-step binding model, the second binding event is more favorable than the first i.e. formation of the homodimer is more favorable than the initial binding of inhibitor to monomeric Sortase A ($K2 > K1$). This reasoning is consistent with previous studies which have demonstrated that Sortase A preferentially forms a homodimer both *in vitro*¹¹ and *in vivo*¹².

We also consider a possible binding mechanism for Actarit binding to Sortase A that happens to exist in homodimer form (Figure 11):

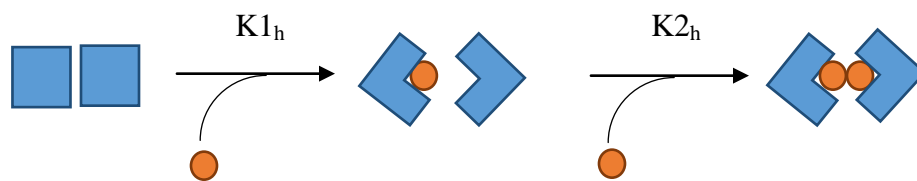


Figure 11.

Two-site sequential binding model for the binding of Actarit (oval) to homodimeric Sortase A (double squares ‘unbound’ and double notched squares ‘bound’). Binding constants for the first and second binding events are $K1_h$ and $K2_h$.

In this case the first binding step would be binding of one molecule of Actarit to one of the two available active sites on the Sortase A homodimer. Binding of the first inhibitor molecule potentially causes a conformational change in the bound part of the homodimer, which in itself may induce the other unbound half to adopt a conformation more susceptible and thus more favorable to binding a second inhibitor molecule. As in the previous model, binding of the second molecule of Actarit is more thermodynamically favorable than binding of the first, as reflected in the data.

It should be noted that the relative orientation of the Sortase A homodimer subunits depicted in the above two figures is arbitrary. It is not known with certainty whether the binding site between Sortase A monomers is located near to or away from their active sites. However, if we have a look at the general distribution of data points in Figure 5, it can be seen that they form a pattern of two connected sigmoid curves. This visualization is redrawn below in Figure 12. It will be noted that the first ten or so data points form the outline of the first sigmoid curve and the remaining points form the second one. Also notable is that the slope of the first sigmoid curve is noticeably greater than that of the second sigmoid curve. What this implies is that the binding properties of the second site (or second binding event) are different from those of the first site (or first binding event), which in turn further suggests that the binding mechanism cannot be characterized as being two independent binding sites. If this were true, we should expect to see a distribution of points forming the outline of two sigmoid curves which are roughly identical both in terms of proportion and slope. As a consequence of this line of reasoning, we believe it is more likely that with respect to the relative orientation of the Sortase A homodimer subunits, each monomer must be facing each other in such a way that their active sites can synergistically influence each other as depicted above in Figure 11. If the Sortase A monomers were forming homodimers with their active sites facing away, then we should not expect to see an ITC binding isotherm featuring two sigmoid curves of differing proportions and slopes.

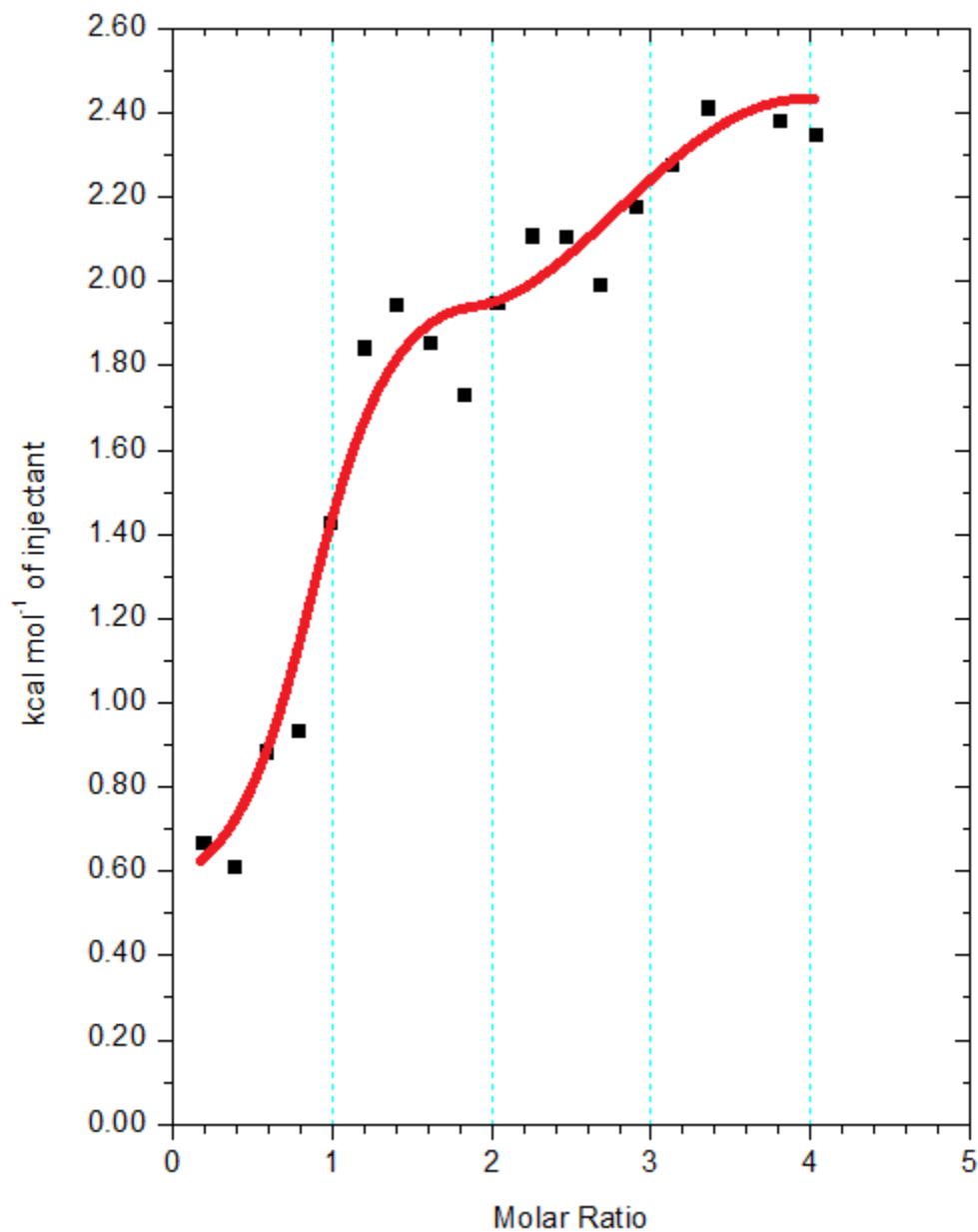


Figure 12.

ITC binding isotherm of Sortase A Δ N59 (19 μ M) and Actarit (380 μ M) at 25°C. Data point corresponding to the 17th of 19 total injections has been removed (See Supplementary Data Figure S1 for full data set). Red line is manually drawn and arbitrarily fitted binding model. This figure is identical to Figure 5 except for removal of boxed calculated values (associated with the fitting of a two-site sequential binding model by the analysis software) and the original fitted model.

This reasoning is consistent with a molecular dynamics simulation study which supported a binding mechanism characterized by conformational selection followed by induced fit¹³. Analysis from the same study also showed that binding of substrate to Sortase A actively affected allosteric pathways in the protein which linked the first and second binding sites, which the authors proposed to be on opposite faces of the protein. Simulation studies of the structure of Sortase A have also shown that its active site undergoes ligand-induced conformational changes and that the actual binding mode may be located away from the active site¹⁴. Interestingly, graphs of the raw experimental ITC data (see Supplementary Data Figure S4 for a representative example) consistently feature both exothermic and endothermic reactions for *every* ligand injection. While further investigation is needed to determine the cause of such phenomena, it is possible that the exothermic portions of the spikes (thermodynamically favorable) correspond to binding of Actarit to Sortase A whilst the endothermic portions of the spikes (thermodynamically unfavorable) correspond to conformational changes within the monomeric protein subunits or interactions between bound monomeric Sortase A.

Given that Sortase A equilibrates between the monomer and homodimer forms¹¹⁻¹², both mechanistic models proposed above must concurrently exist. The changes in enthalpy (ΔH) detected by the ITC machine during the titrations reflect the *total* heat produced by the binding event of each individual titration, whether or not they come from binding of Actarit to the monomer or to the homodimer form of Sortase A. In other words, the measured and calculated data gathered by the ITC machine does not distinguish between binding events happening on the monomer and homodimer fractions of the Sortase A sample. Following this reasoning, the calculated binding constants K1 and K2 reflect the overall chemical properties of the *entire* system. The binding constant K1 would incorporate the first binding events of both mechanisms ($K1 = K1_m + K1_h$), and likewise, the binding constant K2 would incorporate the second binding events of both mechanisms ($K2 = K2_m + K2_h$).

Apart from analysis of hypothetical mechanisms to explain the raw experimental data, results from different ITC experiments demonstrated the importance of optimizing experimental parameters to achieve meaningful results. Figure 8 depicts the results of titrating 1 mM Actarit into 1 μ M Sortase A Δ N59 and is representative of what occurs when the ligand to

macromolecule ratio is very high (approximately 200). While at first glance it appears that calculated values for enthalpy ($\Delta H1$ and $\Delta H2$), entropy ($\Delta S1$ and $\Delta S2$), and binding constants ($K1$ and $K2$) are reasonable, one cannot overlook the possibility that the results are a bogus product of ligand over-saturation and non-specific binding events. It is not possible for any known macromolecule to possess enough unique binding sites to accommodate let alone a fraction of the amount of ligand present in solution. Furthermore, the high concentration of inhibitor used (1 mM) is not biologically relevant in any manner.

Another example of the need to optimize absolute molar concentrations when conducting ITC experiments is shown in Figure 9, an experiment involving 1 μM Sortase A ΔN59 and 5 μM Actarit. Some aspects of this experimental setup can be the cause of potential issues. The final ligand to macromolecule ratio of 1.0 is too low to guarantee sufficient saturation of the macromolecule with ligand. This is particularly true given prior knowledge of the nature of Sortase A and its natural tendency to form dimers. A look at the raw ITC data for this experiment (See Figure S5 in Supplementary Data) shows a wildly fluctuating baseline, which is typical of ITC experiments conducted using very low absolute concentrations of macromolecule. The low ligand to macromolecule ratio is also reflected by the small magnitude of individual spikes (Compare Figure S4 and Figure S5). Referring back to Figure 9, we can see that the data points are randomly scattered (albeit in a general negative trend), and even fitting of the best-fit binding model is done at the cost of an unsettling high value for $\chi^2/\text{degrees of freedom}$ ($1.057 * 10^7!$), indicating a very poor fit.

These two representative examples demonstrate the need to tweak experimental parameters in order to achieve meaningful ITC data which can be interpreted and analyzed. At least for the experiments analyzed previously, we had found through trial and error that concentrations of Actarit and Sortase A ΔN59 resulting in a final ligand to macromolecule ratio of about 4.0 were optimal for producing complete binding isotherms. It was also important that the absolute concentration of Sortase A ΔN59 being used was not any less than 10 μM .

CONCLUSION

In this study we presented an exploratory look at the binding interactions between Sortase A and a small molecule inhibitor deduced through the use of thermodynamic data generated from ITC in corroboration with data from other analytical methods. Application of various binding models to the ITC data suggests that the binding mechanism between Sortase A and inhibitor involves a two-step mechanism featuring induced fit and conformational changes on the part of the protein itself. At the very least, these results rule out the possibility of a one-site or one-step binding mechanism for Sortase A. This finding is consistent with other structural analytical studies which conclude that Sortase A, particularly its active site, undergoes significant conformational change upon binding of ligand. Given that binding of inhibitor (at least for Actarit) to Sortase A homodimer is thermodynamically more favorable than the same binding to the monomer, it is suggested that further development of Sortase A inhibitors be focused on optimization the binding interaction with the homodimer form.

To the best knowledge of the authors, this is the first study of Sortase A involving ITC and shows its feasibility as a valuable analytical method to help study its functional and allosteric mechanisms. Further studies involving other small molecule inhibitors would be worthwhile to evaluate the consistency of the proposed binding mechanisms. This study has also demonstrated that Actarit's *in vitro* dissociation constant is 72 μM . Compared to its IC_{50} value of only 20 μM , this is significantly different, but one has to keep in mind that IC_{50} and K_d values are two different things and at best are only rough approximations of each other. Nevertheless, from a more practicable standpoint, both values are in the mid-micromolar range and are thus medically irrelevant. Other studies of potential Sortase A inhibitors have likewise generated IC_{50} values ranging from the mid- to high-micromolar ranges. This aspect does not preclude them from use as suitable *in vitro* inhibitors for mechanistic and structural studies. Given the largely variable and flexible structure of Sortase A's active site region, it may be worthwhile to develop inhibitors which mimic peptides instead of small molecule inhibitors.

REFERENCES

1. I.M. Gould, Antibiotic resistance: the perfect storm, *Int. J. Antimicrob. Agents* 34 (Suppl. 3) (2009) S2-S5.
2. D.A. Rasko, V. Sperandio, Anti-virulence strategies to combat bacteria-mediated disease, *Nat. Rev. Drug Discov.* 9 (2010) 117-128.
3. L. A. Marraffini, A. C. DeDent, O. Schneewind, Sortases and the art of anchoring proteins to the envelopes of Gram-positive bacteria. *Microbiol. Mol. Bio. Rev.* 70, 192–221 (2006).
4. A.M. Perry, H. Ton-That, S.K. Mazmanian, O. Schneewind, Anchoring of surface proteins to the cell wall of *Staphylococcus aureus*. III. Lipid II is an in vivo peptidoglycan substrate for sortase-catalyzed surface protein anchoring, *J. Biol. Chem.* 277 (2002) 16241-16248.
5. S.K. Mazmanian, G. Liu, E.R. Jensen, E. Lenoy, O. Schneewind, *Staphylococcus aureus* sortase mutants defective in the display of surface proteins and in the pathogenesis of animal infections, *Proc. Natl. Acad. Sci. U. S. A.* 97 (2000) 5510-5515.
6. W.J. Weiss, E. Lenoy, T. Murphy, L. Tardio, P. Burgio, S.J. Projan, et al., Effect of *srtA* and *srtB* gene expression on the virulence of *Staphylococcus aureus* in animal models of infection, *J. Antimicrob. Chemother.* 53 (2004) 480-486.
7. K.-B. Oh, M.-N. Oh, J.-G. Kim, D.-S. Shin, J. Shin, Inhibition of sortase-mediated *Staphylococcus aureus* adhesion to fibronectin via fibronectin-binding protein by sortase inhibitors, *Appl. Microbiol. Biotechnol.* 70 (2006) 102-106.
8. N. Suree, M.E. Jung, R.T. Clubb, Recent advances towards new anti-infective agents that inhibit cell surface protein anchoring in *Staphylococcus aureus* and other gram-positive pathogens, *Mini Rev. Med. Chem.* 7 (2007) 991-1000.
9. S. Cascioferro, M. Totsika, D. Schillaci, Sortase A: An ideal target for anti-virulence drug development, *Microbial Pathogenesis.* 77 (2014) 105-112.
10. Y. Takeba, N. Suzuki, S. Wakisaka, H. Nagafuchi, S. Mihara, A. Kaneko, T. Asai, T. Sakane, Effects of actarit on synovial cell functions in patients with rheumatoid arthritis, *The Journal of rheumatology.* 26 (1999) 25–33.

11. C. Lu, J. Zhu, Y. Want, A. Umeda, R. B. Cowmeadow, E. Lai, G. M. Moreno, M. D. Person, Z. Zhang, Staphylococcus aureus Sortase A Exists as a Dimeric Protein in Vitro, *Biochemistry*. 46 (2007) 9346-9354.
12. J. Zhu, L. Xiang, F. Jiang, Z. Zhang, Equilibrium of sortase A dimerization on Staphylococcus aureus cell surface mediates its cell wall sorting activity, *Exp. Biol. Med.* 241 (2016) 90-100.
13. K. Kappel, J. Wereszczynski, R. T. Clubb, J. A. McCammon, *Protein Science* 21 (2012) 1858-1871.
14. C. Gao, I. Uzelac, J. Gottfries, L. A. Eriksson, Exploration of multiple Sortase A protein conformations in virtual screening, *Scientific Reports* 6 (2016) 1-14.
15. L. Freiburger, K. Auclair, A. Mittermaier, Global ITC fitting methods in studies of protein allostery, *Methods* 76 (2015) 149-161.
16. J. Zhu, C. Lu, M. Standland, E. Lai, G. N. Moreno, A. Umeda, X. Jia, Z. Zhang, Single mutation on the surface of Staphylococcus aureus Sortase A can disrupt its dimerization, *Biochemistry* 47 (2008) 1667-1674.
17. C. P. Guimaraes, M. D. Witte, C. S. Theile, G. Bozkurt, L. Kundrat, A. E. M. Blom, H. L. Ploegh, Site-specific C-terminal and internal loop labeling of proteins using sortase-mediated reactions, *Nature Protocols* 8 (2013) 1787-1799.

SUPPLEMENTARY DATA

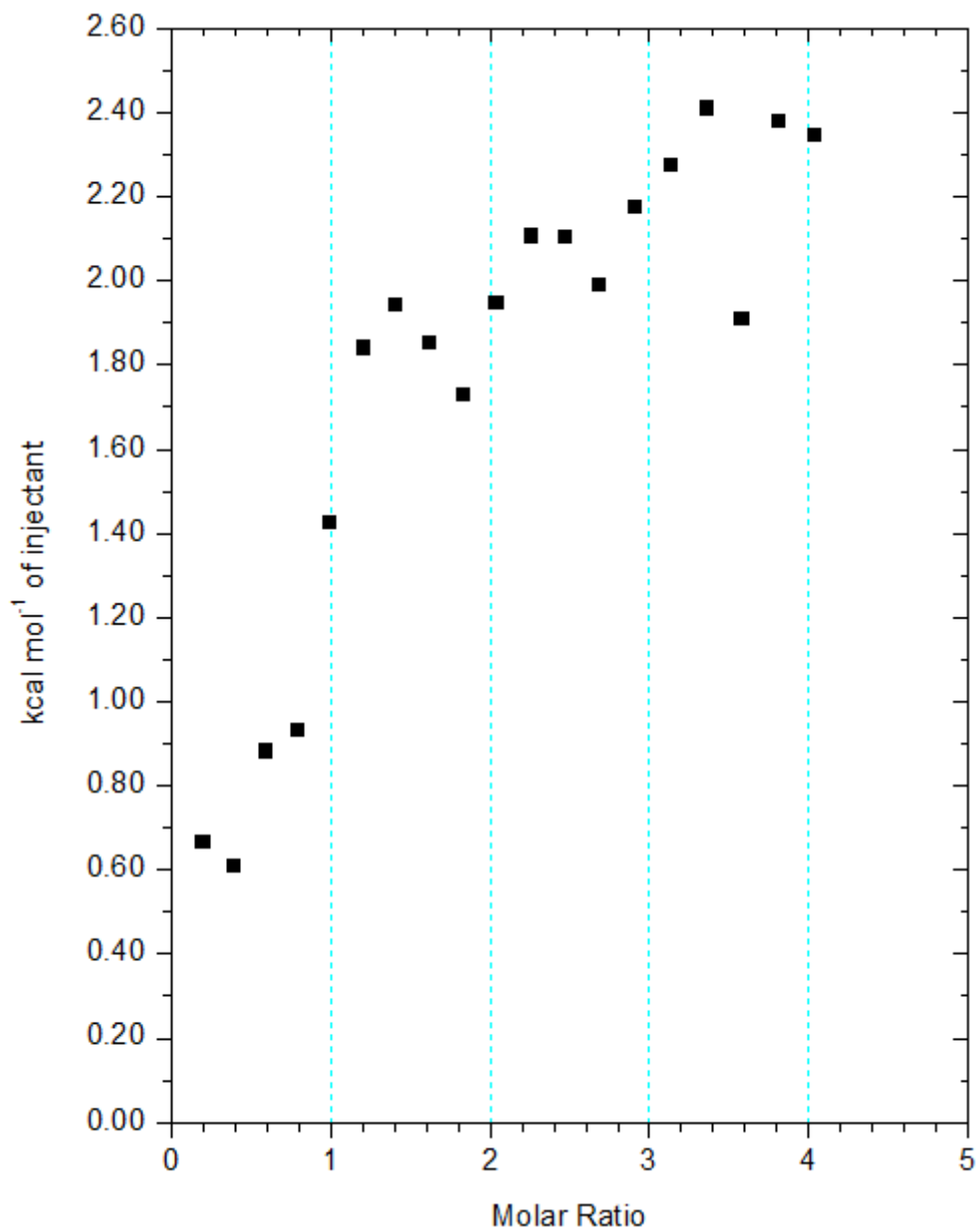


Figure S1.

ITC binding isotherm of Sortase A Δ N59 (19 μ M) and Actarit (380 μ M) at 25°C (first of three experimental repetitions). All original experimental data points are shown.

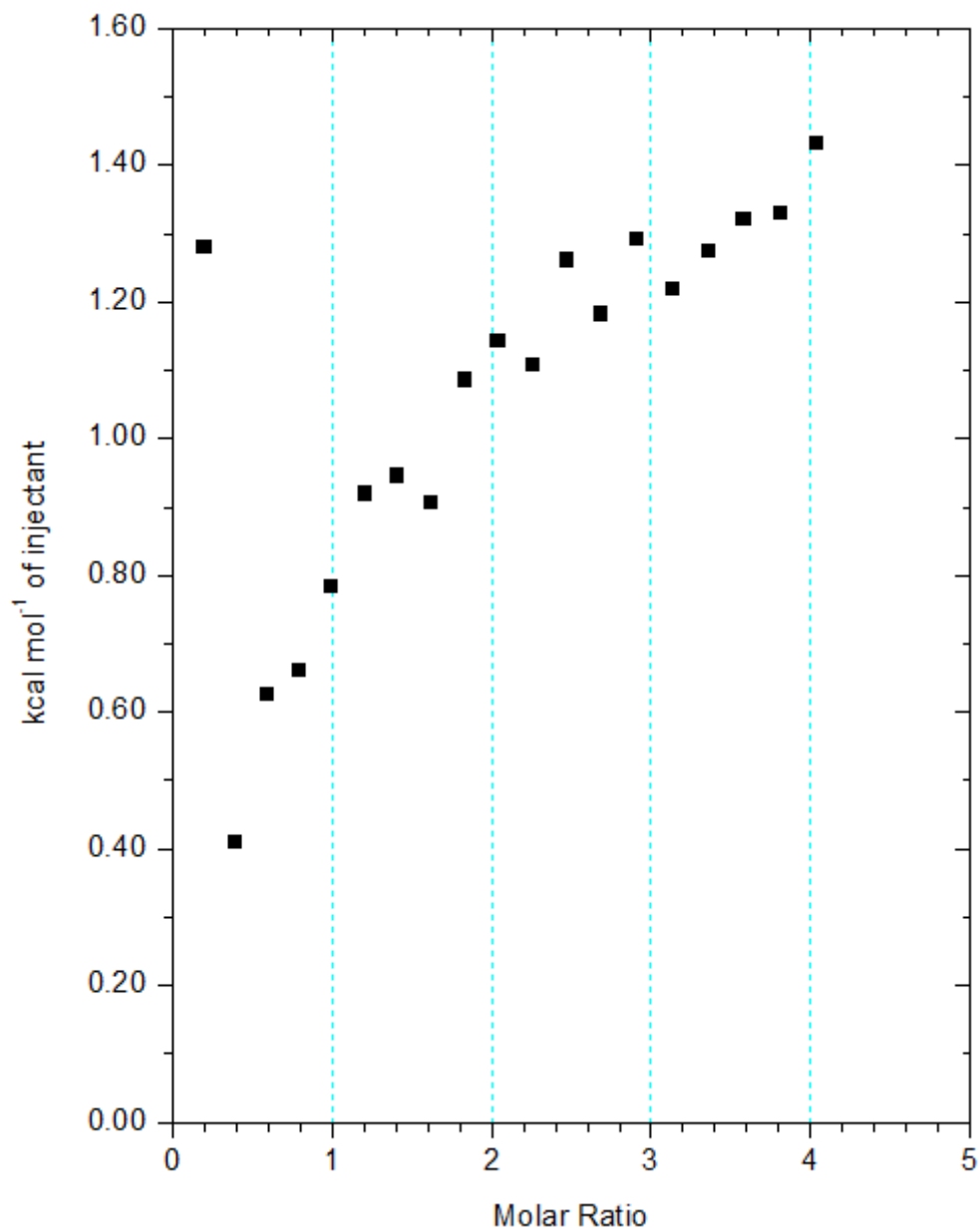


Figure S2.

ITC binding isotherm of Sortase A Δ N59 (19 μ M) and Actarit (380 μ M) at 25°C (second of three experimental repetitions). All original experimental data points are shown.

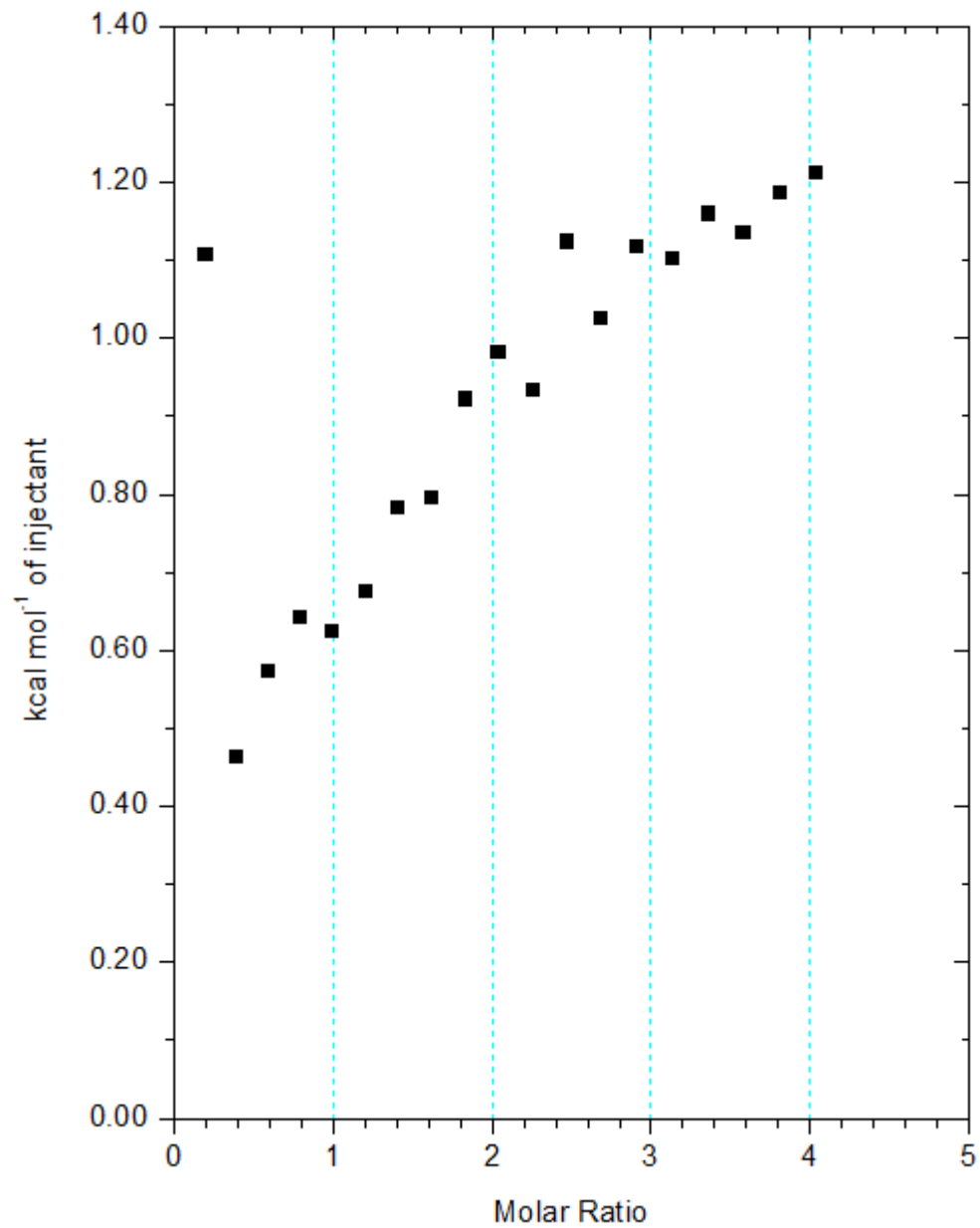


Figure S3.

ITC binding isotherm of Sortase A Δ N59 (19 μ M) and Actarit (380 μ M) at 25°C (third of three experimental repetitions). All original experimental data points are shown.

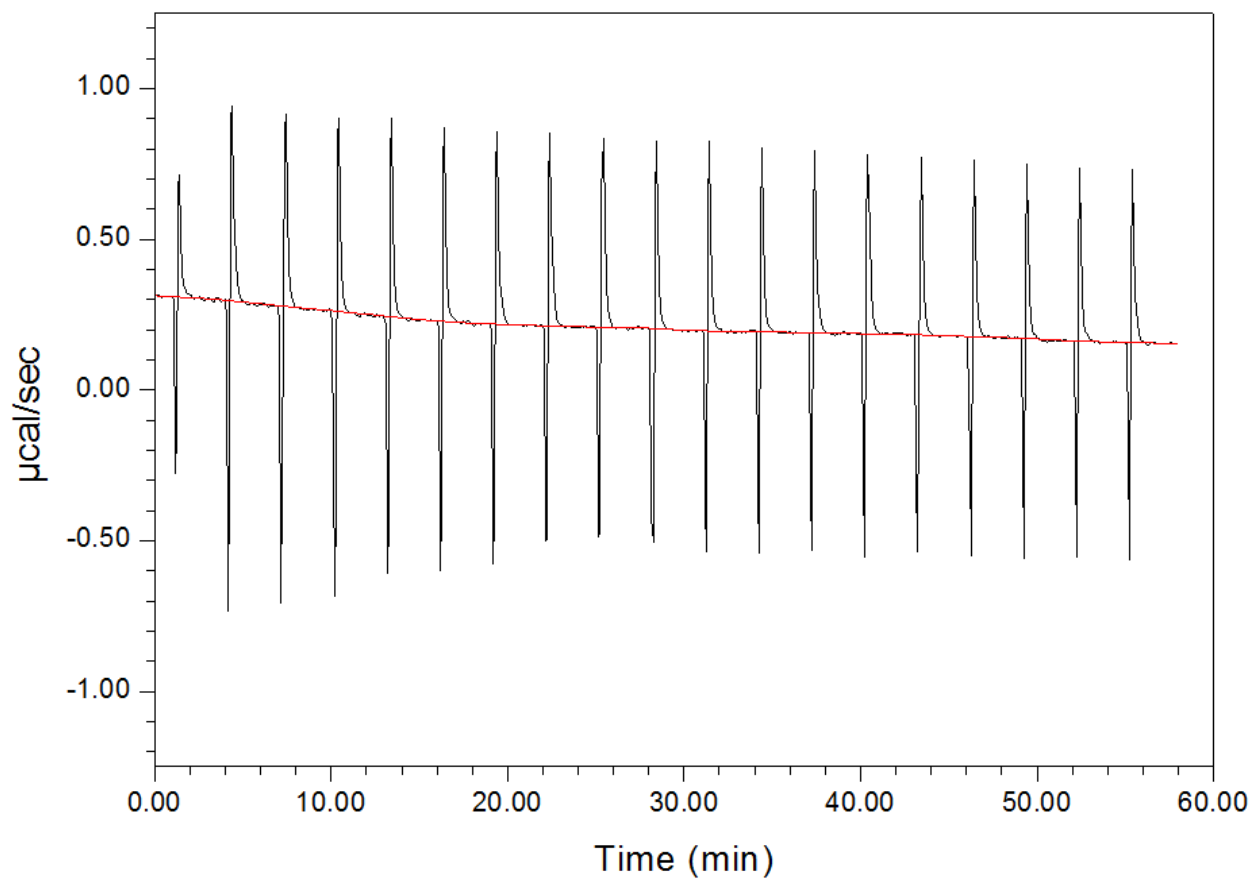


Figure S4.

Representative raw experimental data of ITC experiment with 19 μM Sortase A ΔN59 and 380 μM Actarit. Each spike corresponds to one ligand (Actarit) injection. Baseline reference power is marked in red. Portions of spikes below the baseline reflect exothermic reactions while those above the baseline reflect endothermic reactions.

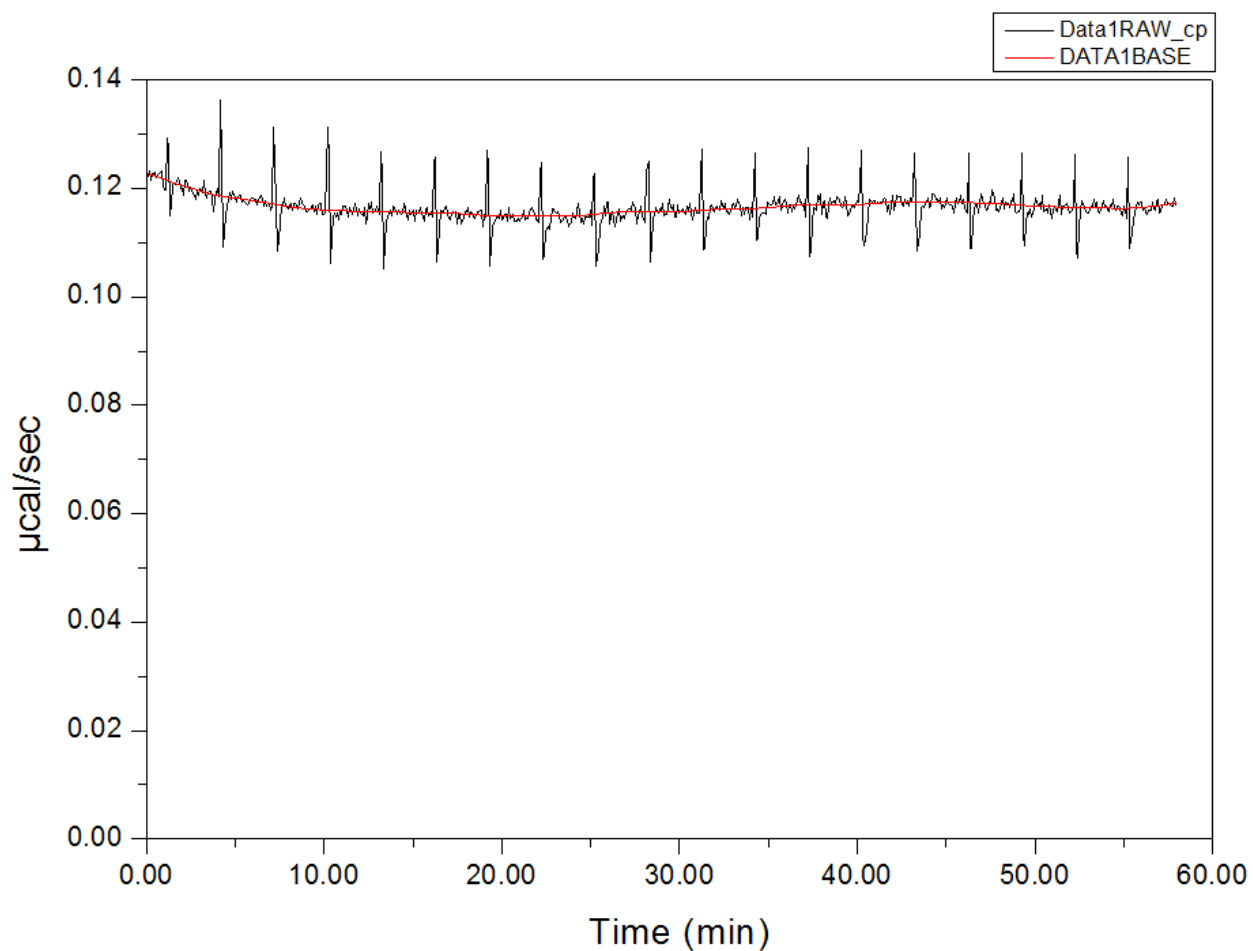


Figure S5.

Raw experimental data of ITC experiment with 1 μM Sortase A ΔN59 and 5 μM Actarit. Each spike corresponds to one ligand (Actarit) injection. Baseline reference power is marked in red. Portions of spikes below the baseline reflect exothermic reactions while those above the baseline reflect endothermic reactions.